Chapter 3

Design of Space-Time Finite Element Methods for Structural Acoustics

In this chapter space-time finite element methods, based on a time-discontinuous variational formulation for fluid-structure interaction, are developed for the solution of the coupled structural acoustics problem in unbounded domains. Throughout this development, the energy estimates obtained in the preceding Chapter are used as a guide for the design of the proposed space-time algorithms. The formulation employs a finite computational fluid domain surrounding the structure and incorporates high-order accurate radiation boundary conditions on the fluid truncation boundary. Non-reflecting boundary conditions are incorporated as 'natural' boundary conditions in the space-time variational equation, i.e. they are enforced weakly in both space and time. An important ingredient for the success of the proposed space-time finite element method is the incorporation of time-discontinuous jump operators that weakly enforce continuity of the solution between space-time slabs. The specific form of these temporal jump operators are designed such that unconditional stability can be proved *a priori* for general unstructured discretizations in both space and time. An algorithm is termed unconditionally stable if in the absence of forcing terms but for arbitrary initial conditions, the computed total structural acoustic energy plus the radiation energy absorbed through the artificial boundary is always less than or equal to the total energy at the previous time step, for arbitrary step sizes. For additional stability, and to prove convergence, least-squares operators based on local residuals of the Euler-Lagrange equations for the coupled system, including the non-reflecting boundary conditions, are incorporated into the space-time formulation.

3.1 Background

Considerable progress has been made in the development of stabilized space-time finite element methods based on a time-discontinuous Galerkin formulation for problems that can be written as a system of first-order equations. As pointed out in the previous Chapter, classical linear acoustics equations can be converted to first-order hyperbolic form and these methods are thus immediately applicable. However, in this approach, the coupled state vector consists of fluid pressure and velocity components, which is computationally uneconomical.

A more direct approach is to develop space-time finite element methods for structural acoustics based on the natural framework of second-order hyperbolic equations for elastodynamics and the acoustic wave equation. Recently, Hughes and Hulbert [1988] and Hulbert and Hughes [1990] have successfully generalized time-discontinuous space-time finite element methods developed for first-order systems to the second-order hyperbolic equations of elastodynamics. In this thesis, the formulation is extended to include both the elastic structure and acoustic fluid posed in second-order hyperbolic form together with their interaction. For the coupled equations, scalar velocity potential ϕ is used as the solution variable for the acoustic fluid, while the displacement vector $\boldsymbol{u}$ is used for the structure. As a consequence of this choice of variables, the coupled variational equations for the fluid and structure give rise to a globally symmetric form, which in the context of the space-time finite element formulation, enables us to prove stability and convergence of the method.

3.2 Overview

The proposed space-time finite element method for the solution of the structural acoustics problem proceeds by considering a partitioning of the space-time domain into space-time slabs. Within each space-time slab we employ a time-discontinuous Galerkin approach, which allows for the use of completely unstructured space-time finite element discretizations and eliminates the need for an additional ordinary differential time integrator. By allowing for solutions to be discontinuous in time, the algorithm proceeds by marching sequentially in time. In Section 3.3 we state the trial and weighting spaces needed for the variational formulation and introduce the concept of the discontinuous jump operator which is critical to the stability of the method. In Section 3.4 the coupled variational equation is stated for the structural acoustics problem including the incorporation of an important class of high-order accurate non-reflecting boundary conditions. In Section 3.5 we introduce the concept of Galerkin/least-squares stabilization, in which least-squares operators are added to the basic Galerkin formulation to enhance the stability, while maintaining the accuracy, of the space-time method. Consistency of the proposed method is exposed in Section 3.6 where the weak enforcement of the Euler-Lagrange equations are discussed. In Section 3.8 we finish up this Chapter with a discussion of the positive form of the resulting space-time matrix equations and issues related to the stability and efficient solution of these equations.

3.3 Finite Element Discretization

The development of the space-time finite element method proceeds by considering an ordered partition of the open time interval, $I =]0, T[$, of the form: $0 = t_0 < t_1 < \ldots < t_N = T$. Denoting the nth open time interval,

$$I_n :=]t_n, t_{n+1}[\tag{3.1}$$

with variable time step $\Delta t_n = t_{n+1} - t_n$ we have $I = \left\{\cup_{n=0}^{N-1} I_n\right\} \cup \{t_1\,,\, t_2\,,\, \ldots, t_{N-1}\}$.

Using this notation,

$$Q_n^s = \Omega_s \times I_n \tag{3.2}$$

$$Q_n^f = \Omega_f \times I_n \tag{3.3}$$

are the nth space-time slabs for the structure and fluid respectively, with boundaries $\Upsilon_n^s = \partial\Omega_s \times I_n$ and $\Upsilon_n^f = \partial\Omega_f \times I_n$. For the nth space-time slab $(n_{el})_n^s$ and $(n_{el})_n^f$ denote the number of space-time finite elements in the subdomains Q_n^s and Q_n^f respectively.

With these definitions, $Q_n^{s^e} \subset Q_n^s$, denotes the interior of the eth element in the structural domain with boundary $\Upsilon_n^{s^e}$. Similarly, $Q_n^{f^e} \subset Q_n^f$, denotes the interior of the eth element in the fluid domain, with boundary $\Upsilon_n^{f^e}$

Figure 3.1 shows an illustration of two consecutive space-time slabs Q_{n-1} and Q_n for the fluid where the superscript is omitted for clarity. Within each space-time element, the trial solution and weighting function are approximated by pth-order polynomials in $\boldsymbol{x}$ and t. These functions are assumed $C^0(Q_n)$ continuous throughout each space-time slab, but are allowed to be discontinuous across the interfaces of the slabs. Assuming the function $\boldsymbol{w}(\boldsymbol{x}\,,\,t)$ to be discontinuous at time t_n, suppressing the argument $\boldsymbol{x}$, the temporal jump operator is defined by,

$$\boxed{[\![\boldsymbol{w}(t_n)]\!] := \boldsymbol{w}(t_n^+) \; - \; \boldsymbol{w}(t_n^-)} \tag{3.4}$$

where

$$\boldsymbol{w}(t_n^{\pm}) = \lim_{\epsilon \to 0\pm} \boldsymbol{w}(t_n + \epsilon)$$

This discontinuity of the finite element functions across space-time slab interfaces, allows for the general use of high-order elements and spectral-type interpolations in both space and time, and provides freedom of changing the spatial discretization from one time step to another.

The collections of finite element interpolation functions are given by the spaces,

Trial structural displacements

$$\mathcal{S}^h = \bigcup_{n=0}^{N-1} \mathcal{S}_n^h\,, \qquad \mathcal{S}_n^h \quad = \quad \left\{ \boldsymbol{u}^h(\boldsymbol{x},t) \middle| \boldsymbol{u}^h \in (C^0(Q_n^s))^d\,,\, \boldsymbol{u}^h\Big|_{Q_n^{s^e}} \in (\mathcal{P}^p(Q_n^{s^e}))^d \right\}$$

Trial fluid potential

$$\mathcal{T}^h = \bigcup_{n=0}^{N-1} \mathcal{T}_n^h\,, \qquad \mathcal{T}_n^h \quad = \quad \left\{ \phi^h(\boldsymbol{x},t) \middle| \phi^h \in C^0(Q_n^f)\,,\, \phi^h\Big|_{Q_n^{f^e}} \in \mathcal{P}^p(Q_n^{f^e}) \right\}$$

where $\mathcal{P}^p$ denotes the space of pth-order polynomials, C^0 denotes the space of continuous functions and d is the number of space dimensions.

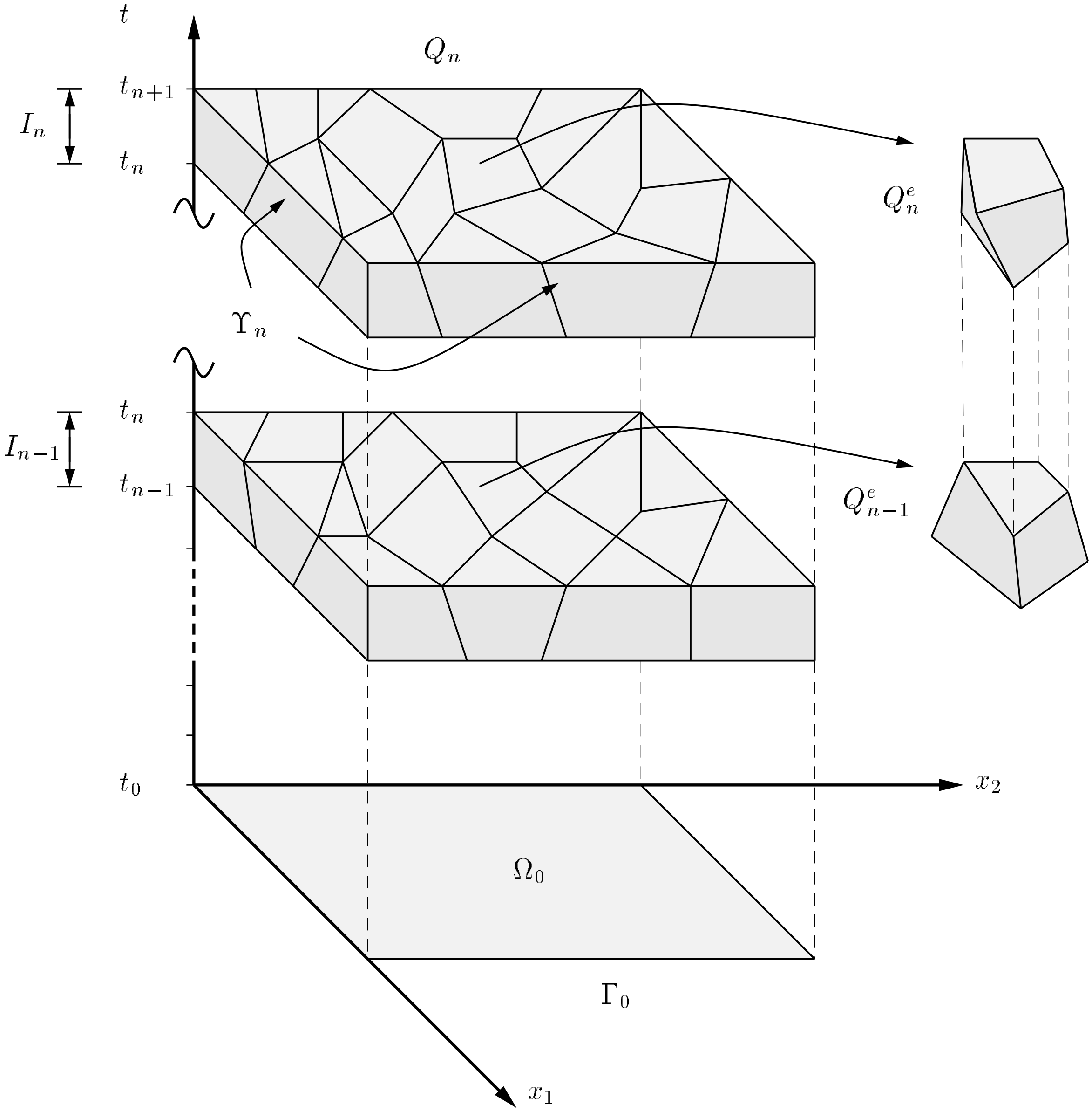

Figure 3.1: Illustration of two consecutive space-time slabs with unstructured finite element meshes in space-time.

As noted earlier, for clarity of presentation, prescribed displacements and prescribed velocity potential boundary conditions were not defined, i.e. essential boundary conditions are omitted. As a result of this assumption, the formulation is simplified in that the trial spaces and weighting spaces are identical, i.e. $\mathcal{S}^h = \mathcal{V}^h$ and $\mathcal{T}^h = \mathcal{W}^h$. Inclusion of essential boundary conditions is straightforward with the usual restrictions placed on the trial and weighting spaces.

3.4 Discontinuous Galerkin Formulation

The space-time variational formulation for the coupled structural acoustics problem is obtained from a weighted residual of the governing equations (2.27)–(2.33) within a space-time slab and incorporates time-discontinuous jump terms across slab interfaces. The specific form of this variational equation is designed such that *a priori* stability and energy estimates analogous to those described in Theorem 2.1 for the continuum problem are obtained for the discrete problem.

Preliminaries:

Before stating the space-time variational equations, it is useful to introduce the following notation.

$$\tilde{Q}_n = \bigcup_{e=1}^{(n_{el})_n} Q_n^e \qquad \text{(element interiors)} \tag{3.5}$$

$$\tilde{\Upsilon}_n = \bigcup_{e=1}^{(n_{el})_n} \Upsilon_n^e - \Upsilon_n \qquad \text{(interior mesh boundaries)} \tag{3.6}$$

Space-time element boundaries which coincide with the artificial boundary $(\Upsilon_\infty)_n = \Gamma_\infty \times I_n$ are denoted, $(\bar{\Upsilon}_\infty)_n^e = \Upsilon_n^e \cap (\Upsilon_\infty)_n$, where the overbar indicates the closure. Using this notation, the interiors of the element boundaries restricted to the artificial boundary are defined as,

$$(\tilde{\Upsilon}_\infty)_n = \bigcup_{e=1}^{(n_{el})_n} (\Upsilon_\infty)_n^e \tag{3.7}$$

Other notations are the following standard inner products,

$$(\boldsymbol{w}^h\,,\,\boldsymbol{u}^h)_{\Omega_s} = \int_{\Omega_s} \boldsymbol{w}^h \cdot \boldsymbol{u}^h \, d\Omega \tag{3.8}$$

$$a(\boldsymbol{w}^h\,,\,\boldsymbol{u}^h)_{\Omega_s} = \int_{\Omega_s} \nabla \boldsymbol{w}^h \cdot \boldsymbol{\sigma}(\nabla \boldsymbol{u}^h) \, d\Omega \tag{3.9}$$

$$(w^h\,,\,\phi^h)_{\Omega_f} = \int_{\Omega} \rho_0 \, w^h \, \phi^h \, d\Omega \tag{3.10}$$

$$(\nabla w^h\,,\,\nabla \phi^h)_{\Omega_f} = \int_{\Omega} \rho_0 \, \nabla w^h \cdot \nabla \phi^h \, d\Omega \tag{3.11}$$

$$(w^h\,,\,\phi^h)_{\Gamma_\infty} = \int_{\Gamma_\infty} \rho_0 \, w^h \, \phi^h \, d\Gamma \tag{3.12}$$

$$(w^h\,,\,\phi^h)_{Q_n^f} = \int_{t_n}^{t_{n+1}} (w^h\,,\,\phi^h)_{\Omega_f} \, dt \tag{3.13}$$

$$(w^h\,,\,\phi^h)_{(\Upsilon_\infty)_n} = \int_{t_n}^{t_{n+1}} (w^h\,,\,\phi^h)_{\Gamma_\infty} \, dt \tag{3.14}$$

$$(w^h\,,\,\phi^h)_{\tilde{Q}_n^f} = \sum_{e=1}^{(n_{el})_n} \int_{Q_n^{f^e}} w^h \phi^h \, dQ \tag{3.15}$$

The strain-energy inner product for the structure is denoted by (3.9) while the kinetic energy inner product for the fluid is denoted by (3.11). Note that inner products for the fluid are weighted by the fluid reference density ρ_0. The meaning of other similar notations may be inferred from these.

3.4.1 Variational Equations

In this section the time-discontinuous Galerkin variational equations for the coupled fluid-structure interaction problem are stated.

Within each space-time slab, $n = 0, 1, ..., N-1$, the object is to find $\boldsymbol{\chi}^h := \{\boldsymbol{u}^h\,,\,\phi^h\} \in \mathcal{S}_n^h \times \mathcal{T}_n^h$, such that $\forall\ \boldsymbol{\psi}^h := \{\boldsymbol{w}^h\,,\,w^h\} \in \mathcal{V}_n^h \times \mathcal{W}_n^h$, the following coupled variational equations are satisfied,

$$B_s(\boldsymbol{w}^h\,,\,\boldsymbol{\chi}^h)_n = L_s(\boldsymbol{w}^h)_n \tag{3.16}$$

$$B_f(w^h\,,\,\boldsymbol{\chi}^h)_n \quad = \quad L_f(w^h)_n \tag{3.17}$$

$$B_s(\boldsymbol{w}^h\,,\,\boldsymbol{\chi}^h)_n \;:=\; E_s(\boldsymbol{w}^h\,,\,\boldsymbol{u}^h)_n \,-\, A(\boldsymbol{w}^h\,,\,\phi^h\boldsymbol{n})_n \tag{3.18}$$

$$B_f(w^h\,,\,\boldsymbol{\chi}^h)_n \;:=\; E_f(w^h\,,\,\phi^h)_n \,+\, A(\boldsymbol{u}^h\,,\,w^h\boldsymbol{n})_n \,+\, E_r(w^h\,,\,\phi^h)_n \tag{3.19}$$

with the following definitions,

$$\begin{aligned} E_s(\boldsymbol{w}^h\,,\,\boldsymbol{u}^h)_n \;:=\;& (\dot{\boldsymbol{w}}^h\,,\,\rho_s\ddot{\boldsymbol{u}}^h)_{Q_n^s} \,+\, a(\dot{\boldsymbol{w}}^h\,,\,\boldsymbol{u}^h)_{Q_n^s} \\ +\;& (\dot{\boldsymbol{w}}^h(t_n^+)\,,\,\rho_s\dot{\boldsymbol{u}}^h(t_n^+))_{\Omega_s} \,+\, a(\boldsymbol{w}^h(t_n^+)\,,\,\boldsymbol{u}^h(t_n^+))_{\Omega_s} \end{aligned} \tag{3.20}$$

$$\begin{aligned} E_f(w^h\,,\,\phi^h)_n \;:=\;& (\dot{w}^h\,,\,a^2\ddot{\phi}^h)_{Q_n^f} \,+\, (\nabla\dot{w}^h\,,\,\nabla\phi^h)_{Q_n^f} \\ +\;& (\dot{w}^h(t_n^+)\,,\,a^2\,\dot{\phi}^h(t_n^+))_{\Omega_f} \,+\, (\nabla w^h(t_n^+)\,,\,\nabla\phi^h(t_n^+))_{\Omega_f} \end{aligned} \tag{3.21}$$

$$A(\boldsymbol{w}^h\,,\,\phi^h\boldsymbol{n})_n \;:=\; (\dot{\boldsymbol{w}}^h\,,\,\rho_0\,\dot{\phi}^h\boldsymbol{n})_{(\Upsilon_i)_n} \tag{3.22}$$

$$\begin{aligned} L_s(\boldsymbol{w}^h)_n \;:=\;& (\dot{\boldsymbol{w}}^h\,,\,\bar{\boldsymbol{t}})_{(\Upsilon_\sigma)_n} \\ +\;& (\dot{\boldsymbol{w}}^h(t_n^+)\,,\,\rho_s\dot{\boldsymbol{u}}^h(t_n^-))_{\Omega_s} \,+\, a(\boldsymbol{w}^h(t_n^+)\,,\,\boldsymbol{u}^h(t_n^-))_{\Omega_s} \end{aligned} \tag{3.23}$$

$$\begin{aligned} L_f(w^h)_n \;:=\;& (\dot{w}^h\,,\,f)_{Q_n^f} \\ +\;& (\dot{w}^h(t_n^+)\,,\,a^2\,\dot{\phi}^h(t_n^-))_{\Omega_f} \,+\, (\nabla w^h(t_n^+)\,,\,\nabla\phi^h(t_n^-))_{\Omega_f} \end{aligned} \tag{3.24}$$

The operator $E_r(w^h\,,\,\phi^h)_n$, incorporates the time-dependent non-reflecting boundary operators $\mathbb{S}_m$ as natural boundary conditions, i.e., they are enforced weakly through integration over both the artificial boundary Γ_∞ and the time interval I_n. The formal definition of this boundary operator with details for the implementation of the non-reflecting boundary conditions are given in the next section.

In order to guarantee a stable space-time finite element algorithm, the coupled variational equations (3.16) and (3.17) are constructed in a form which is consistent with the energy (stability) estimates given in Lemma 2.1 and Theorem 2.1 The design criteria then is to construct a coupled variational equation such that the natural energy norm emanating from this variational equation satisfies a stability (energy) identity analogous to that obtained for the continuum problem. A key feature is the use of the time derivative (time rate of change) of $\boldsymbol{\psi}^h$, i.e. $\dot{\boldsymbol{\psi}}^h := \{\dot{\boldsymbol{w}}^h\,,\,\dot{w}^h\}$, as the weighting function in the terms evaluated over Q_n in (3.20) and (3.21). With this choice of weighting function, the form of these terms are consistent with the time rate of change of structural acoustic energy defined in (2.47) – (2.49). In the operator $E_s(\cdot\,,\,\cdot)_n$, the terms evaluated over Q_n^s, act to weakly enforce the momentum balance in the structure while in $E_f(\cdot\,,\,\cdot)_n$, the terms evaluated over Q_n^f, act to weakly enforce the scalar wave equation in the fluid within the interior of the nth space-time slab.

The terms evaluated over the structural domain Ω_s in (3.20) and (3.23), together with the terms evaluated over the fluid domain Ω_f in (3.21) and (3.24) act to weakly enforce continuity across space-time slab interfaces. Figure 3.2 illustrates the weak enforcement of the velocity $\boldsymbol{v}^h = \nabla\phi^h$ and pressure $p^h = -\rho_0\dot{\phi}^h$ for the acoustic fluid through the temporal jump operators associated with (3.21) and (3.24), i.e.

$$\boxed{(\dot{w}^h(t_n^+)\,,\,a^2\;\underbrace{[\![\dot{\phi}^h(t_n)]\!])_{\Omega_f}}_{\text{pressure jump}}\;+(\nabla w^h(t_n^+)\,,\,\underbrace{[\![\nabla\phi^h(t_n)]\!])_{\Omega_f}}_{\text{velocity jump}}}$$

Similar temporal jump operators associated with (3.20) and (3.23) defined over Ω_s act to weakly enforce structural velocities and stresses across time steps. The specific form of these jump operators are designed such that continuity is weakly enforced via a kinetic and strain energy inner product for the structure and similarly a kinetic and potential energy inner product for the acoustic fluid. These jump conditions are the mechanism by which information is advanced from one space-time slab to the next. Physically, they add a consistent numerical dissipation into the algorithm which helps control any oscillations that may occur in the vicinity of discontinuities or sharp gradients in the solution.

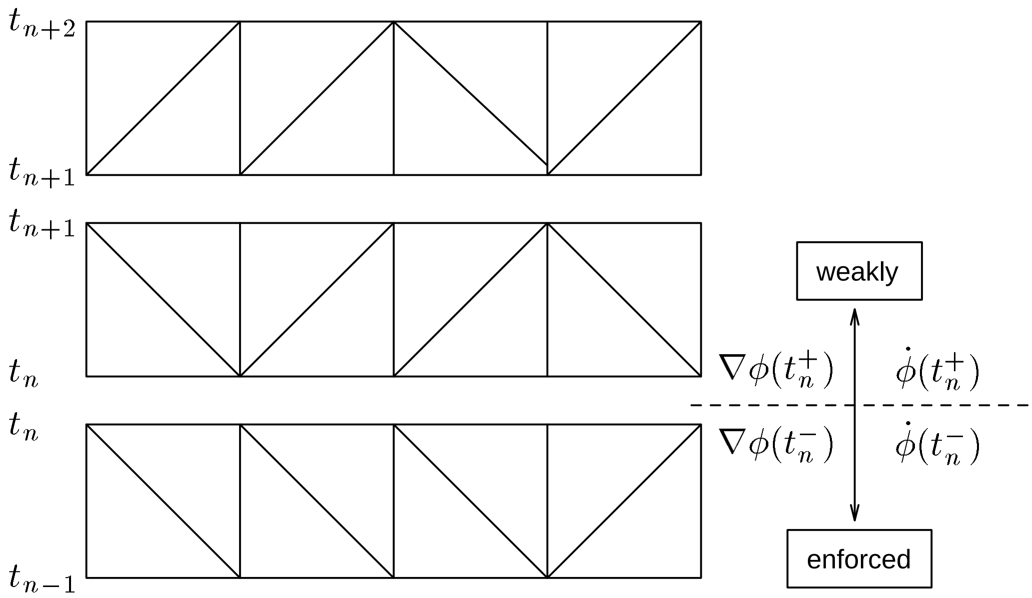

Figure 3.2: Illustration of weak enforcement of velocity $\mathrm{v} = \nabla\phi$ and pressure $p = -\rho_0\dot{\phi}$ for the acoustic fluid across space-time slab interfaces.

Fluid-structure interaction is accomplished through the coupling operators $A(\cdot\,,\,\cdot)_n$ integrated over the fluid-structure interface $(\Upsilon_i)_n = \Gamma_i \times I_n$. These coupling terms appearing in (3.18) and (3.19) weakly enforce the acoustic pressure interface condition (2.5) and continuity of normal velocity condition (2.20), respectively. The fact that the coupling operators in both (3.18) and (3.19) are of the same form; namely (3.22), follows directly from the choice of $\boldsymbol{\mathcal{X}}^h := \{\boldsymbol{u}^h\,,\,\phi^h\}$ for the structure-fluid solution variables and the consistent weighting $\dot{\boldsymbol{\psi}}^h := \{\dot{\boldsymbol{w}}^h\,,\,\dot{w}^h\}$. This global symmetry property of the coupled space-time variational equations facilitates the establishment of stability and convergence proofs for the coupled finite element formulation in a manner similar to that obtained for the continuum problem.

Remarks

1. If pressure is used as the solution variable for the fluid, then the interface boundary condition (2.21) relating the normal pressure gradient to the structural accelerations must be used in place of (2.20). As a result, the coupling terms in the variational equation *will not* be of the same form and would destroy

the global symmetry of the coupled system. As a consequence, it is difficult (if not impossible) to guarantee unconditional stability for unstructured space-time meshes. Recall that a similar difficulty was found for the continuum problem.

2. The method is applied in one space-time slab at a time; data from the end of the previous slab are employed as initial conditions for the current slab. Because the solution is weakly enforced across slab interfaces, the finite element mesh may change from one slab to the next and it is not required that the meshes match across the discrete time levels. This is especially useful for adaptive schemes where the finite element discretization can be refined/unrefined within space-time slabs to track wave fronts as they propagate along space-time characteristics.

3.4.2 Non-Reflecting Boundary Conditions

To allow for a large number of alternative definitions for the non-reflecting boundary conditions, the linear mapping $\mathbb{S}_m\phi$ defined previously in (2.22) is assumed to take the following general abstract form,

$$\boxed{\mathbb{S}_m\phi = \sum_{j=0}^{m} C_j \left[\frac{\partial^j \phi}{\partial t^j}\right] \qquad \text{on} \quad \Upsilon_\infty := \Gamma_\infty \times I_n} \tag{3.25}$$

In this expression, the index m reflects the order of the temporal derivatives appearing in the operator, and C_j , $j = 0, 1, \dots m$, are spatial operators that may be local differential operators that couple only adjacent points on the artificial boundary, or nonlocal integral operators that couple all points on the artificial boundary Γ_∞. Specific examples of time-dependent non-reflecting boundary conditions which can be expressed in this general form are discussed in detail in Chapter 5 for problems in $\mathbb{R}^3$, and Chapter 6 for problems in $\mathbb{R}^2$. Here we note that the first-order operator ($m = 1$) defined previously in (2.26) conform to this representation with the spatial operators C_j , $j = 0, 1$ reducing to $1/R$, and $1/c$.

In general, boundary conditions of the form (3.25) provide increasing accuracy with the order m; however, as the order increases, they become increasingly difficult to implement in a standard semidiscrete finite element setting due to the occurrence

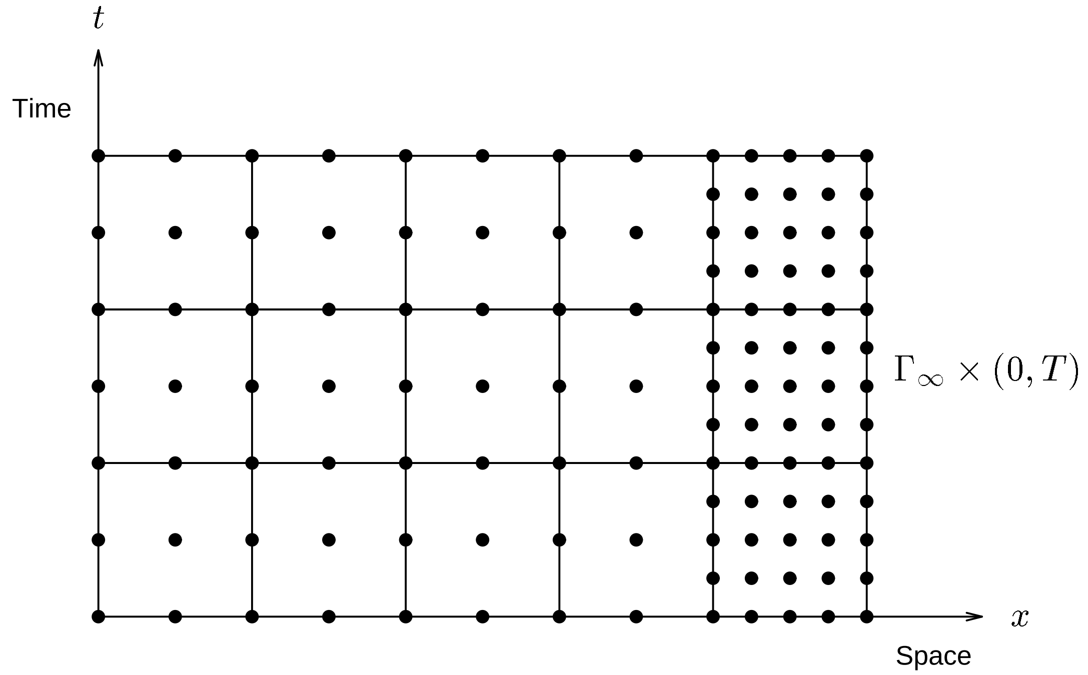

Figure 3.3: Illustration of space-time discretization where the temporal interpolation is increased from biquadratic to biquartic in the region of the non-reflecting boundary $\Gamma_\infty \times]0,T[$.

of high-order time derivatives on the truncation boundary Υ_∞. Semidiscrete methods for second-order hyperbolic wave equations, which discretize the spatial domain with finite elements, lead to a second-order system of ordinary differential equations in time. These ordinary differential equations are then integrated using standard finite difference algorithms such as the Newmark family of time integrators. Since standard semidiscrete algorithms are restricted to integrating up to second-order time derivatives, they are limited to orders $m \leq 2$ only.

Space-time finite element methods, in which the solution is allowed to be discontinuous across space-time slabs places no restriction as to the order m of time derivative appearing in the operator $\mathbb{S}_m$. Since continuity is enforced weakly between time steps, standard C^0 continuous interpolation functions in the time coordinate can be used up to the order dictated by the operator $\mathbb{S}_m$. Figure 3.3 illustrates how the order of the temporal interpolation in the space-time formulation can be increased in the region of the boundary conditions so that temporal accuracy is locally increased to a level required by the boundary condition. It is this special property of the discontinuous Galerkin formulation that provides for the potential to implement (3.25) up to any order desired. It is noted however, that high-order non-reflecting boundary conditions beyond second-order may involve high-order spatial derivatives in C_j, that require increased continuity in the spatial coordinate. In this case special local boundary elements which incorporate high-order continuous spatial basis functions would be needed.

While in principle, it is possible to implement the time dependent operators to any order desired to obtain a greater accuracy, it is difficult to prove *a priori* unconditional stability for orders $m \geq 3$. In the discussion to follow we describe how the time-discontinuous Galerkin space-time method provides a natural variational setting for the incorporation of non-reflecting boundary conditions of the form (3.25), and how under certain conditions on the boundary operators stability and convergence can be proved.

In this work, the class of non-reflecting boundary operators defined in (3.25) are incorporated into the space-time finite element method as 'natural' boundary conditions, i.e., they are enforced weakly in space-time. For boundary operators up to second-order ($m = 2$), the bilinear form $E_r(\cdot\,,\,\cdot)_n$ appearing in the space-time variational equation (3.19), is defined as,

$$\begin{aligned} E_r(w^h\,,\,\phi^h)_n \quad &:= \quad (\dot{w}^h\,,\,\mathbb{S}_m\phi^h)_{(\Upsilon_\infty)_n} \\ &+ \quad d_2(\dot{w}^h(t_n^+)\,,\,\underbrace{[\![\dot{\phi}^h(t_n)]\!]}_{\text{jump}})_{\Gamma_\infty} + d_0(w^h(t_n^+)\,,\,\underbrace{[\![\phi^h(t_n)]\!]}_{\text{jump}})_{\Gamma_\infty} \end{aligned} \tag{3.26}$$

The term evaluated over $(\Upsilon_\infty)_n := \Gamma_\infty \times I_n$ acts to weakly enforce the non-reflecting boundary condition (3.25) over the time interval $]t_n\,,\,t_{n+1}[$ and Γ_∞. The form of this boundary operator is guided by the definition of the acoustic intensity given in (2.46). Replacing the trial solution with w^h, we have

$$\begin{aligned} (\dot{w}^h\,,\,\mathbb{S}_m w^h)_{(\Upsilon_\infty)_n} \quad &= \quad \int_{t_n}^{t_{n+1}} \mathcal{D}(w^h)\ dt \\ &= \quad \int_{t_n}^{t_{n+1}} \int_{\Gamma_\infty} \rho_0 \dot{w}^h \mathbb{S}_m w^h \ d\Gamma\ dt \end{aligned} \tag{3.27}$$

Comparing this result to (2.46) we conclude that this term represents an acoustic radiation inner product integrated over the time interval I_n.

As a specific example, consider the first-order, ($m = 1$), non-reflecting boundary condition defined previously in (2.26) and repeated here as,

$$\mathbb{S}_1\phi = C_0\phi + C_1\dot{\phi} \tag{3.28}$$

where the spatial operators reduce to the positive values $C_1 = 1/R$ and $C_2 = 1/c$. For this case, the acoustic radiation operator takes the form,

$$\boxed{(\dot{w}^h\,,\,\mathbb{S}_1\phi^h)_{(\Upsilon_\infty)_n} := \quad d_0(\dot{w}^h\,,\,\phi^h)_{(\Upsilon_\infty)_n} + d_1(\dot{w}^h\,,\,\dot{\phi}^h)_{(\Upsilon_\infty)_n}} \tag{3.29}$$

where the index on the bilinear operators d_1 and d_2 reflects the order of the time derivative appearing on the trial solution. For this simple case, the bilinear operators reduce to,

$$d_0(\dot{w}^h\,,\,\phi^h)_{(\Upsilon_\infty)_n} \quad = \quad \frac{1}{R}\int_{t_n}^{t_{n+1}}\int_{\Gamma_\infty}\rho_0\,\dot{w}^h\;\phi^h\;d\Gamma\;dt \tag{3.30}$$

$$d_1(\dot{w}^h\,,\,\dot{\phi}^h)_{(\Upsilon_\infty)_n} \quad = \quad \frac{1}{c}\int_{t_n}^{t_{n+1}}\int_{\Gamma_\infty}\rho_0\,\dot{w}^h\;\dot{\phi}^h\;d\Gamma\;dt \tag{3.31}$$

Similarly, extending the sequence (3.25) to second-order ($m = 2$),

$$\mathbb{S}_2\phi = C_0\phi + C_1\dot{\phi} + C_2\ddot{\phi} \tag{3.32}$$

the radiation operator reduces to,

$$\boxed{(\dot{w}^h\,,\,\mathbb{S}_2\phi^h)_{(\Upsilon_\infty)_n} := \quad d_0(\dot{w}^h\,,\,\phi^h)_{(\Upsilon_\infty)_n} + d_1(\dot{w}^h\,,\,\dot{\phi}^h)_{(\Upsilon_\infty)_n} + d_2(\dot{w}^h\,,\,\ddot{\phi}^h)_{(\Upsilon_\infty)_n}} \tag{3.33}$$

The form of the bilinear operators d_j depends on the local or non-local character of the spatial operators C_j appearing in (3.25). The index for the operators d_j , $j = 0, 1, 2$, reflects the order of the time derivative on the trial solution appearing in the operator. Specific examples for $\mathbb{S}_2$ will be given in Chapters 5 and 6.

The terms evaluated over the space-time slab interface at the boundary Γ_∞ in (3.26) act to weakly enforce continuity of the trial solution across space-time slab interfaces. The specific form of these operators are designed such that continuity at the artificial boundary Γ_∞ is weakly enforced in a form which is consistent with the radiation boundary term evaluated over $(\Upsilon_\infty)_n$. Thus the form of the consistent temporal jump operators $[\![\phi^h(t_n)]\!]$ and $[\![\dot{\phi}^h(t_n)]\!]$ embedded in the last two terms of (3.26) depend on the form of the spatial derivatives appearing in the bilinear operators $d_0(\cdot\,,\,\cdot)_{\Gamma_\infty}$ and $d_2(\cdot\,,\,\cdot)_{\Gamma_\infty}$. These consistent temporal jump operators are required in order to ensure that the discontinuous Galerkin solution is unconditional stability and are the crucial element that enable generalization of the space-time finite element method to handle exterior domains. Note that no jump operator is needed for the term corresponding to $d_1(\dot{w}^h\,,\,\dot{\phi}^h)_{(\Upsilon_\infty)_n}$. The reason for this becomes clear from the stability analysis described in the next chapter where it is shown that this term naturally leads to a well-defined norm, requiring no additional stabilization.

For the first-order non-reflecting boundary condition defined in (2.26), second-order time derivatives do not appear, and as a result, the term d_2 is not present in the radiation boundary integral. Thus the only consistent jump operator needed is,

$$d_0(w^h(t_n^+)\,,\,[\![\phi^h(t_n)]\!])_{\Gamma_\infty} \quad = \quad \frac{1}{R}\int_{\Gamma_\infty} \rho_0\, w^h(t_n^+)\,,\,[\![\phi^h(t_n)]\!]\; d\Gamma \tag{3.34}$$

Remarks

1. Since the boundary condition $\mathbb{S}_1$ is a local (differential) operator in both space and time, when implemented with standard finite element interpolations with compact support, the boundary integrals couple only degrees-of-freedom in adjacent elements, and the banded sparse data structure of the space-time finite element arrays are preserved. Examples of local non-reflecting boundary conditions of second-order $\mathbb{S}_2$, will be given in Chapters 5 and 6.

2. To facilitate the stability and convergence proofs incorporating non-reflecting boundary conditions, boundary operators are assumed to be spatially non-negative, i.e.,

$$d_j(w^h\,,\,w^h)_{\Gamma_\infty} \geq 0\,, \quad j = 0, 1, 2 \qquad \forall\, w^h \in \mathcal{W}^h \tag{3.35}$$

Boundary operators which satisfy this positive definite property form an important class of operators. This class of operators also serve as a basic framework for the analysis of other boundary operators, such as those involving unsymmetric terms.

Examining the boundary operators defined in (3.30) and (3.31) for $\mathbb{S}_1$, it is clear that these operators satisfy condition (3.35) explicitly, i.e.

$$d_0(w^h\,,\,w^h)_{\Gamma_\infty} \;=\; c_0||w^h||^2_{\Gamma_\infty} \geq 0 \tag{3.36}$$

$$d_1(w^h\,,\,w^h)_{\Gamma_\infty} \;=\; c_1||w^h||^2_{\Gamma_\infty} \geq 0 \tag{3.37}$$

where $c_0 = 1/R$ and $c_1 = 1/c$ are positive constants, with notation for the weighted L_2 norm on the boundary,

$$||w^h||^2_{\Gamma_\infty} := \int_{\Gamma_\infty} \rho_0 (w^h)^2 \; d\Gamma \tag{3.38}$$

3.5 Galerkin/Least-Squares Stabilization

In order to enhance the stability of the basic time-discontinuous Galerkin space-time formulation, and to facilitate the proof that the method converges for arbitrary space-time discretizations, local residuals of the governing differential equations in the form of least-squares operators are added to the variational equations. Stabilized methods of this type are referred to as Galerkin/least-squares (GLS) methods. GLS methods were originally developed to improve the stability of numerical solutions for the advection-diffusion equation Hughes, Franca, and Hulbert [1989], and the Euler and Navier-Stokes equations Shakib, Hughes, and Johan [1991]. These ideas have since been extended to second-order hyperbolic equations in the context of elastodynamics in Hughes and Hulbert [1988] and Hulbert and Hughes [1990]. In this section, we extend the use of GLS stabilization to the coupled fluid-structure interaction problem including the incorporation of non-reflecting boundaries. The time-discontinuous Galerkin/least-squares (GLS) formulation for structural acoustics is stated formally as:

Within each space-time slab, $n = 0, 1, ..., N-1$; Find $\boldsymbol{\mathcal{X}}^h := \{\boldsymbol{u}^h\,,\,\phi^h\} \in \mathcal{S}^h_n \times \mathcal{T}^h_n$, such that $\forall\ \boldsymbol{\psi}^h := \{\boldsymbol{w}^h\,,\, w^h\} \in \mathcal{V}_n^h \times \mathcal{W}_n^h$,

$$B^s_{GLS}(\boldsymbol{w}^h\,,\,\boldsymbol{\chi}^h)_n \quad = \quad L^s_{GLS}(\boldsymbol{w}^h)_n \tag{3.39}$$

$$B^f_{GLS}(w^h\,,\,\boldsymbol{\chi}^h)_n \quad = \quad L^f_{GLS}(w^h)_n \tag{3.40}$$

where

$$B^s_{GLS}(\boldsymbol{w}^h\,,\,\boldsymbol{\chi}^h)_n \quad = \quad B_s(\boldsymbol{w}^h\,,\,\boldsymbol{\chi}^h)_n + B^s_{LS}(\boldsymbol{w}^h\,,\,\boldsymbol{\chi}^h)_n \tag{3.41}$$

$$L^s_{GLS}(\boldsymbol{w}^h)_n \quad = \quad L_s(\boldsymbol{w}^h)_n + L^s_{LS}(\boldsymbol{w}^h)_n \tag{3.42}$$

similarly,

$$B^f_{GLS}(w^h\,,\,\boldsymbol{\chi}^h)_n \quad = \quad B_f(w^h\,,\,\boldsymbol{\chi}^h)_n + B^f_{LS}(w^h\,,\,\boldsymbol{\chi}^h)_n \tag{3.43}$$

$$L^f_{GLS}(w^h)_n \quad = \quad L_f(w^h)_n + L^f_{LS}(w^h)_n \tag{3.44}$$

The least-squares addition to the Galerkin variational equations are defined as:

$$\begin{aligned}
B^s_{LS}(\boldsymbol{w}^h\,,\,\boldsymbol{\chi}^h)_n \quad := \quad & (\mathcal{L}_s\boldsymbol{w}^h\,,\,\rho_s^{-1}\boldsymbol{\tau}\mathcal{L}_s\boldsymbol{u}^h)_{\tilde{Q}^s_n} \\
+ \quad & ([\![\boldsymbol{\sigma}(\nabla\boldsymbol{w}^h)(\boldsymbol{x})]\!]\cdot\boldsymbol{n}\,,\,\rho_s^{-1}\boldsymbol{s}[\![\boldsymbol{\sigma}(\nabla\boldsymbol{u}^h)(\boldsymbol{x})]\!]\cdot\boldsymbol{n})_{\tilde{\Upsilon}^s_n} \\
+ \quad & (\boldsymbol{\sigma}(\nabla\boldsymbol{w}^h)\cdot\boldsymbol{n}\,,\,\rho_s^{-1}\boldsymbol{s}\boldsymbol{\sigma}(\nabla\boldsymbol{u}^h)\cdot\boldsymbol{n})_{(\Upsilon_\sigma)_n} \\
+ \quad & (\mathcal{L}_1\boldsymbol{\psi}^h\,,\,\rho_s^{-1}\boldsymbol{s}\mathcal{L}_1\boldsymbol{\chi}^h)_{(\Upsilon_i)_n}
\end{aligned} \tag{3.45}$$

$$L^s_{LS}(\boldsymbol{w}^h)_n \quad := \quad (\boldsymbol{\sigma}(\nabla\boldsymbol{w}^h)\cdot\boldsymbol{n}\,,\,\rho_s^{-1}\boldsymbol{s}\,\bar{\boldsymbol{t}})_{(\Upsilon_\sigma)_n} \tag{3.46}$$

and

$$\begin{aligned}
B^f_{LS}(w^h\,,\,\boldsymbol{\chi}^h)_n \quad := \quad & (\mathcal{L}_f w^h\,,\,c^2\tau\mathcal{L}_f\phi^h)_{\tilde{Q}^f_n} \\
+ \quad & (\mathcal{L}_r w^h\,,\,c^2 s\mathcal{L}_r\phi^h)_{(\tilde{\Upsilon}_\infty)_n} \\
+ \quad & ([\![w^h_{,n}(\boldsymbol{x})]\!]\,,\,c^2 s[\![\phi^h_{,n}(\boldsymbol{x})]\!])_{\tilde{\Upsilon}^f_n}
\end{aligned}$$

$$+ \quad (\mathcal{L}_2 \boldsymbol{\psi}^h \,,\, c^2 s \mathcal{L}_2 \boldsymbol{\chi}^h)_{(\Upsilon_i)_n} \tag{3.47}$$

$$L^f_{LS}(w^h)_n \quad := \quad (\mathcal{L}_f w^h \,,\, c^2 \tau f)_{\tilde{Q}^f_n} \tag{3.48}$$

In the above expressions we define:

$$\mathcal{L}_s \boldsymbol{u}^h \quad := \quad \rho_s \ddot{\boldsymbol{u}}^h - \nabla \cdot \boldsymbol{\sigma}(\nabla \boldsymbol{u}^h) \tag{3.49}$$

$$\mathcal{L}_f \phi^h \quad := \quad a^2 \ddot{\phi}^h - \nabla^2 \phi^h \tag{3.50}$$

$$\mathcal{L}_r \phi^h \quad := \quad \phi^h_{,n} + \mathbb{S}_m \phi^h \tag{3.51}$$

$$\mathcal{L}_1 \boldsymbol{\chi}^h \quad := \quad \boldsymbol{\sigma}(\nabla \boldsymbol{u}^h) \cdot \boldsymbol{n} - \rho_0 \dot{\phi}^h \boldsymbol{n} \tag{3.52}$$

$$\mathcal{L}_2 \boldsymbol{\chi}^h \quad := \quad \dot{\boldsymbol{u}}^h \cdot \boldsymbol{n} - \phi^h_{,n} \tag{3.53}$$

and the normal derivative is denoted $\phi^h_{,n} = \nabla \phi^h \cdot \boldsymbol{n}$. The scalar parameters τ and s, are local weighting parameters for the fluid equations designed to improve stability without degrading the accuracy of the underlying time-discontinuous Galerkin method. The GLS parameter τ has dimensions of time and can be interpreted as an intrinsic time-scale, while the parameter s has dimensions of inverse speed and is referred to as a slowness scale. Similarly for the structure, $\boldsymbol{\tau}$ and $\boldsymbol{s}$ are intrinsic time scale and slowness matrices respectively; both are of size $d \times d$, Hughes and Hulbert [1988].

From a Fourier analysis of the time-discontinuous method Shakib and Hughes [1991a], it was shown that the Galerkin/least-squares formulation achieves high-order accuracy and eliminates undesirable high frequency response without introducing excessive algorithmic damping in the low frequency regime. The GLS weighting parameters are mesh dependent functions that may vary from element-to-element, and when set to zero, the formulation specializes to the discontinuous Galerkin method. Both slowness and time scale parameters are needed in the convergence proof. However, from an algorithmic point of view, the implementation of the terms involving the slowness parameters involve unconventional and possibly expensive calculations. Numerical experience in Hulbert [1989] and Chapter 4 of this thesis indicate that optimal convergence rates are achieved even with the omission of the slowness parameters, and therefore in practice, these parameters are set to zero, i.e. $s = 0$ and $\boldsymbol{s} = \mathbf{0}$.

Remarks

1. Galerkin/least-squares methods have also been used to enhance the stability and accuracy of solutions to the related reduced wave equation (Helmholtz equation) governing time-harmonic acoustics in the frequency domain, see HARARI AND HUGHES [1991b,1992c], THOMPSON AND PINSKY [1993c,1993d]; details are given in Chapter 8.

2. For numerical solutions exhibiting sharp gradients or discontinuities due to shocks, nonlinear discontinuity capturing operators are available to help further control oscillations that may occur in the solution, HULBERT [1992]. However, for the majority of linear structural acoustics problems, numerical experience has indicated that the added expense resulting from a nonlinear solve as required from the use of these discontinuity capturing operators is not justified.

3.6 Euler-Lagrange equations

Weak enforcement of the governing Euler-Lagrange equations for the structure is exposed by integrating (3.39) by parts to yield the following weighted residual expression,

$$
\begin{aligned}
0 \quad &= \quad B^s_{GLS}(\boldsymbol{w}^h\,,\,\boldsymbol{\mathcal{X}}^h)_n \;-\; L^s_{GLS}(\boldsymbol{w}^h)_n \\
&= \quad (\dot{\boldsymbol{w}}^h + \rho_s^{-1}\boldsymbol{\tau}\mathcal{L}_s\boldsymbol{w}^h\,,\,\boldsymbol{r}^h_s)_{\tilde{Q}^s_n} \\
&\quad + \quad (\dot{\boldsymbol{w}}^h + \rho_s^{-1}\boldsymbol{s}\boldsymbol{\sigma}(\nabla\boldsymbol{w}^h)\cdot\boldsymbol{n}\,,\,\boldsymbol{\sigma}(\nabla\boldsymbol{u}^h)\cdot\boldsymbol{n} - \bar{\boldsymbol{t}})_{(\Upsilon_\sigma)_n} \\
&\quad + \quad (\dot{\boldsymbol{w}}^h + \rho_s^{-1}\boldsymbol{s}[\![\boldsymbol{\sigma}(\nabla\boldsymbol{w}^h)(\boldsymbol{x})]\!]\cdot\boldsymbol{n}\,,\,[\![\boldsymbol{\sigma}(\nabla\boldsymbol{u}^h)(\boldsymbol{x})]\!]\cdot\boldsymbol{n})_{(\tilde{\Upsilon}^s)_n} \\
&\quad + \quad (\dot{\boldsymbol{w}}^h + \rho_s^{-1}\boldsymbol{s}\mathcal{L}_1\boldsymbol{\psi}\,,\,\boldsymbol{r}^h_1)_{(\Upsilon_i)_n} \\
&\quad + \quad (\dot{\boldsymbol{w}}^h(t_n^+)\,,\,[\![\dot{\boldsymbol{u}}^h(t_n)]\!])_{\Omega_s}
\end{aligned}
$$

$$+ \quad a(\boldsymbol{w}^h(t_n^+)\,,\,[\![\boldsymbol{u}^h(t_n)]\!])_{\Omega_s} \tag{3.54}$$

where

$$\begin{array}{lcll} \boldsymbol{r}_s^h & = & \boldsymbol{\mathcal{L}}_s \boldsymbol{u}^h & \text{(equation of motion)} \\ \boldsymbol{r}_1^h & = & \boldsymbol{\mathcal{L}}_1 \boldsymbol{\chi}^h & \text{(coupling boundary condition)} \end{array} \tag{3.55}$$

The second line in (3.54) describes the weak enforcement of the momentum balance residual $\boldsymbol{r}_s^h$, for the structure within a space-time slab; the third line acts to weakly enforce the prescribed traction at the boundary Γ_σ; while the terms in line four define the weak enforcement of the traction continuity across element boundaries. This term arises from integration-by-parts over the spatial domain. Line five describes the weak enforcement of the traction coupling boundary condition $\boldsymbol{r}_1^h$, at the interface between the structure and the fluid. The last two lines in (3.54) show how continuity between space-time slab interfaces is weakly enforced via a total structural energy inner product.

Similarly for the fluid, integrating (3.40) by parts yields,

$$\begin{aligned} 0 \quad &= \quad B_{GLS}^f(w^h\,,\,\boldsymbol{\chi}^h)_n \;-\; L_{GLS}^f(w^h)_n \\ &= \quad (\dot{w}^h + \tau c^2 \boldsymbol{\mathcal{L}}_f w^h\,,\, r_f^h)_{\tilde{Q}_n^f} \\ &+ \quad (\dot{w}^h + s c^2 \boldsymbol{\mathcal{L}}_r w^h\,,\, r_\infty^h)_{(\tilde{\Upsilon}_\infty)_n} \\ &+ \quad (\dot{w}^h + s c^2 [\![w_{,n}^h(\boldsymbol{x})]\!]\,,\,[\![\phi_{,n}^h(\boldsymbol{x})]\!])_{(\tilde{\Upsilon}^f)_n} \\ &+ \quad (\dot{w}^h + s c^2 \boldsymbol{\mathcal{L}}_2 \boldsymbol{\psi}\,,\, r_2^h)_{(\Upsilon_i)_n} \\ &+ \quad (\dot{w}^h(t_n^+)\,,\, a^2\,[\![\dot{\phi}^h(t_n)]\!])_{\Omega_f} \\ &+ \quad (\nabla w^h(t_n^+)\,,\,[\![\nabla \phi^h(t_n)]\!])_{\Omega_f} \\ &+ \quad d_2(\dot{w}^h(t_n^+)\,,\,[\![\dot{\phi}^h(t_n)]\!])_{\Gamma_\infty} \\ &+ \quad d_0(w^h(t_n^+)\,,\,[\![\phi^h(t_n)]\!])_{\Gamma_\infty} \end{aligned} \tag{3.56}$$

where

$$\begin{aligned} r_f^h &= \mathcal{L}_f \phi^h - f && \text{(wave equation)} \\ r_\infty^h &= \mathcal{L}_r \phi^h && \text{(radiation boundary condition)} \\ r_2^h &= \mathcal{L}_2 \boldsymbol{\mathcal{X}}^h && \text{(coupling boundary condition)} \end{aligned} \tag{3.57}$$

The second line in (3.56) describes the weak enforcement of the wave equation r_f^h, over the space-time slab; the third line acts to weakly enforce the non-reflecting boundary conditions r_∞^h, at the artificial boundary; while the terms in line four define the weak enforcement of the gradient continuity in space. This term arises from integration-by-parts over the space-time domain. The notation $[\![\phi_{,n}^h(\boldsymbol{x})]\!] = \phi_{,n}^h(\boldsymbol{x}^+ , t) - \phi_{,n}^h(\boldsymbol{x}^- , t)$ is defined as the spatial jump in the gradient across element boundaries. Line five describes the weak enforcement of the kinematic coupling boundary condition r_2^h at the interface between the fluid and the structure.

The last four lines in (3.56) show how continuity of the solution is weakly enforced across space-time slabs through the temporal jump operators. Within the domain Ω_f, continuity is weakly enforced via a total acoustic energy inner product. At the artificial boundary Γ_∞, continuity is weakly enforced via the radiation boundary operators $d_2(\cdot\,,\,\cdot)_{\Gamma_\infty}$ and $d_0(\cdot\,,\,\cdot)_{\Gamma_\infty}$. These additional operators are needed in order to ensure stability and are the crucial element that enable generalization of the time-discontinuous space-time finite element method to handle non-reflecting boundary conditions. In Chapter 6, an example is given which demonstrates how the solution may become unstable if these jump terms are not included on Γ_∞.

3.7 Consistency

From (3.54) and (3.56), it follows that a sufficiently smooth exact solution $\boldsymbol{\mathcal{X}} := (\boldsymbol{u}\,,\,\phi)$, to the initial/boundary-value problem (2.27)–(2.33), satisfies the coupled GLS variational equations:

$$B_{GLS}^s(\boldsymbol{w}^h\,,\,\boldsymbol{\mathcal{X}})_n = L_{GLS}^s(\boldsymbol{w}^h)_n \tag{3.58}$$

$$B_{GLS}^f(w^h\,,\,\boldsymbol{\mathcal{X}})_n = L_{GLS}^f(w^h)_n \tag{3.59}$$

$\forall\, \boldsymbol{\psi} := \{\boldsymbol{w}^h\,,\, w^h\} \in \mathcal{V}_n^h \times \mathcal{W}_n^h$ and $n = 0, 1, ..., N-1$. Thus the error in the finite element solution is orthogonal with respect to the operators,

$$B^s_{GLS}(\boldsymbol{w}^h\,,\,\boldsymbol{E})_n \quad = \quad 0 \tag{3.60}$$

$$B^f_{GLS}(w^h\,,\,\boldsymbol{E})_n \quad = \quad 0 \tag{3.61}$$

where $\boldsymbol{E} = \boldsymbol{\mathcal{X}}^h - \boldsymbol{\mathcal{X}}$ is the error; in components $\boldsymbol{E} = \{\boldsymbol{u}^h - \boldsymbol{u}\,,\, \phi^h - \phi\}$. This consistency condition is necessary for maintaining optimal convergence rates for higher-order finite element space-time interpolations. Clearly the time-discontinuous Galerkin formulation with $(\boldsymbol{\tau} = 0, \boldsymbol{s} = 0)$ and/or $(\tau = 0\,, s = 0)$ also satisfies a consistency condition.

3.8 Space-Time Matrix Equations

The space-time matrix equations are obtained by introducing space-time approximations for the structural displacement $\boldsymbol{u}^h$, and acoustic velocity potential ϕ^h,

$$\begin{aligned} \boldsymbol{u}^h(\boldsymbol{x}, t) &= \boldsymbol{N}^e_s(\boldsymbol{x}, t)\, \boldsymbol{d}^e \quad \in \quad \boldsymbol{C}^0(\Omega_s \times I_n) \\ \phi^h(\boldsymbol{x}, t) &= \boldsymbol{N}^e_f(\boldsymbol{x}, t)\, \boldsymbol{\phi}^e \quad \in \quad C^0(\Omega_f \times I_n) \end{aligned}$$

where $\boldsymbol{N}^e_s(\boldsymbol{x}, t) \in Q^s_n$ and $\boldsymbol{N}^e_f(\boldsymbol{x}, t) \in Q^f_n$ are the e^{th} element shape functions for the structure and fluid respectively, and $\boldsymbol{d}^e$ and $\boldsymbol{\phi}^e$ are the element structure displacement and fluid velocity potential solution vectors. Recall that these piecewise element shape functions are C^0 continuous within the space-time slab, but are allowed to be discontinuous across time slabs. Introduction of these approximations into the space-time variational equations (3.39) and (3.40), leads directly to the following coupled system of algebraic equations to be solved in sequence for each time interval $I_n =]t_n\,,\, t_{n+1}[, \quad n = 0\,,\, 1\,,\, \cdots N-1$:

$$\begin{bmatrix} \boldsymbol{K}_s & -\boldsymbol{A} \\ \boldsymbol{A}^T & \boldsymbol{K}_f + \boldsymbol{K}_r \end{bmatrix} \begin{Bmatrix} \boldsymbol{d} \\ \boldsymbol{\phi} \end{Bmatrix} = \begin{Bmatrix} \boldsymbol{f}_s \\ \boldsymbol{f}_f \end{Bmatrix} \tag{3.62}$$

where $\boldsymbol{d}$ and $\boldsymbol{\phi}$ are the global solution vectors for time interval I_n. In the above system, $\boldsymbol{K}_s$ and $\boldsymbol{K}_f$ are the positive matrices emanating from the structural operator

E_s and the fluid operator E_f defined in (3.20) and (3.21) respectively; together with additional least-squares terms. The positive matrix $\boldsymbol{K}_r$ emanates from the positive non-reflecting boundary operators E_r defined in (3.26). The fluid-structure coupling matrix $\boldsymbol{A}$ is given by,

$$\boxed{\boldsymbol{A} \;=\; \mathop{\mathbf{A}}_{e=1}^{n_{el}} \int_{t_n}^{t_{n+1}} \int_{\Gamma_i^e} \rho_f \boldsymbol{N}_{s,t}^{eT} \boldsymbol{n} \boldsymbol{N}_{f,t}^{e} \; d\Gamma^e \; dt} \tag{3.63}$$

where n_{el} is the number of elements in the nth space-time slab, $\mathop{\mathbf{A}}_{e=1}^{n_{el}}$ denotes the assembly operator and the comma with subscript t on the finite element interpolations indicates the time derivative. Note that different space-time interpolations for the fluid domain Q_n^f and the structural domain Q_n^s can be accommodated, allowing possible combinations such as cubic interpolation for the fluid, and quadratic interpolation in the structure.

As a consequence of the choice of $\boldsymbol{\chi}^h := \{\boldsymbol{u}^h\,,\,\phi^h\}$ variables, the matrix equations emanating from the coupled space-time formulation for the structure-fluid interaction problem take on a positive form. This property follows directly from the global symmetry of the coupled variational equations and is intimately related to the stability of the algorithm. The prove of unconditional stability for the coupled system will be given in the next chapter. The algorithm is termed unconditionally stable if, in the absence of forcing terms but for arbitrary initial conditions, then the computed total energy for the system plus the radiation energy absorbed through the artificial boundary is always less than or equal to the total energy at the previous time step for arbitrary step-sizes.

In general, space-time methods give rise to a larger system of equations than those produced by typical semidiscrete methods. In this work, solutions to the numerical examples given in Chapters 5 and 6 were obtained using a direct Crout elimination solver with profile storage and dynamic memory allocation, see HUGHES [1987] Chap.11. Profile reduction based on a modified version of the reverse CUTHILL-MCKEE algorithm was used to minimize storage, (see Algorithm 582 in ACM-Trans. Math. Software, Vol. 8, No. 2.) For larger problems, iterative strategies such as the Generalized Minimum Residual (GMRES) algorithms used by SHAKIB et al. [1989], and JOHAN et al. [1991], for matrices arising in computational fluid dynamics may be needed.

In order to decrease the computational cost associated with the use of the space-time method, the coupled system of equations may be cast in predictor-corrector form, where multiple corrector passes would be used to solve a reduced number of equations, SHAKIB,HUGHES, JOHAN [1991b]. This strategy reduces the system of equations to a sequence of smaller systems within each space-time slab, where iterative strategies may be used for their solution. HULBERT [1989] successfully developed a strategy for generating predictor-multicorrector algorithms for the time-discontinuous Galerkin method for second-order hyperbolic equations; however there is some difficulty extending this idea to the space-time Galerkin/least-squares method in multi-dimensions.

A further strategy for the coupled structural acoustics problem is the use of fractional-step (staggered) solution algorithms. In this approach, a modular computer implementation would be used with separate fluid and structural analyzers interfaced through the coupling terms. The integration process would then be carried out in alternating stages: The solution of either the fluid or the structural system would be advanced first, then the other system would be solved following a time extrapolation of the coupling terms as forcing functions. Previous researchers have used staggered schemes for structural acoustics in the context of Galerkin semidiscrete finite element methods using acoustic pressure and structural displacement variables, see PARK AND FELIPPA [1989]. However, do to the somewhat 'ad hoc' coupling used in these formulations, standard staggered methods are only conditionally stable, and additional stabilizing terms are typically required in an attempt to 'patch-up' the deficiencies in these methods. It is anticipated that as a result of the firm mathematical framework inherent in the time-discontinuous Galerkin finite element method presented in this work, a staggered (fractional-step) space-time method can be obtained which inherits the good stability of the underlying method. Another approach that may prove useful for the solution of the structural acoustics problem is the class of fractional-step procedures developed in ARMERO [1993]. In any approach to coupling the acoustic fluid and shell structure it is essential that the consistency and stability of the method be maintained.

3.9 Conclusions

In this chapter, a new space-time finite element formulation for transient fluid-structure interaction based on the time-discontinuous Galerkin method for second-order hyperbolic systems, Hughes and Hulbert [1988], has been presented. The method is developed from a space-time variational equation for the coupled problem of structural acoustics in $\boldsymbol{\mathcal{X}} = \{\boldsymbol{u}\,,\,\phi\}$ variables including the incorporation of a class on high-order non-reflecting boundary conditions. As a consequence of this choice of variables, the coupled variational equations inherit the stability (energy) properties of the continuum problem, which in the context of the coupled space-time finite element equations, leads to a positive matrix form. In the next Chapter, these properties are exploited in a stability analysis where we prove that the proposed space-time method for structural acoustics is unconditionally stable for general unstructured space-time meshes.